

# A NOISE PRESERVING SHARPENING FILTER FOR CT IMAGE ENHANCEMENT

*Madhuri Nagare<sup>1</sup>      Jie Tang<sup>2</sup>      Obaidullah Rahman<sup>3</sup>      Brian Nett<sup>2</sup>  
 Roman Melnyk<sup>2</sup>      Ken D. Sauer<sup>3</sup>      Charles A. Bouman<sup>1</sup>*

<sup>1</sup>School of Electrical and Computer Engineering, Purdue University, West Lafayette, IN, USA 47907

<sup>2</sup>GE Healthcare, Waukesha, WI, USA 53188

<sup>3</sup>Department of Electrical Engineering, University of Notre Dame, Notre Dame, IN, USA 46556

## ABSTRACT

There is growing interest in employing deep neural networks (DNN) for image sharpening. However, sharpening medical computed tomography (CT) images is challenging because sharpening substantially amplifies high-frequency noise. Alternatively, sharpening algorithms that are also designed to denoise produce images lacking texture. Most importantly, radiologists strongly prefer reading images at a consistent level of noise. Hence it is preferable that a sharpening algorithm not substantially change the noise energy or texture.

In this work, we propose a noise preserving sharpening filter (NPSF) to sharpen CT images while keeping the noise energy and texture in the result similar to that of the input. We achieve this by adding appropriately scaled noise while training. Furthermore, the NPSF is characterized by three user-adjustable parameters which give flexibility to achieve a desired level of sharpness and noise. Our experiments show that the NPSF can sharpen noisy images while producing desired noise level and texture.

**Index Terms**— Low-dose CT, deblurring, large focal spot CT, deep neural networks

## 1. INTRODUCTION

Medical CT image sharpening is challenging due to the noise-resolution trade-off. Li et al. showed in [1] that for a linear reconstruction kernel, noise variance increases by  $f^4$  if the spatial resolution is increased  $f$  times along all the dimensions. The noise increases further for high-resolution kernels [2]. Hence a variety of methods developed for sharpening in the literature also employ some kind of denoising.

Model based iterative reconstruction (MBIR) algorithms provide good spatial resolution and noise reduction [3, 4]. However, they tend to be computationally expensive. An alternative approach is to improve resolution in either the sinogram [5] or image domain [6].

Recently, convolutional neural networks (CNNs) have been among the most popular methods for image resolution

enhancement [7]. CNN based methods either implement a two-step process of sharpening and denoising [6, 8] or train a single network for both tasks [9, 10]. However, due to the noise-resolution trade-off [1], the algorithm performing both tasks simultaneously may not be optimal [6]. Furthermore, networks with embedded denoising are computationally expensive, require more hyperparameter tuning, and most importantly, they tend to produce images that lack texture which is critical in clinical applications [11, 12].

A generative adversarial network (GAN) can improve the texture in the sharpened images [13]. However, GANs could also possibly add inaccurate or even unreal image detail.

In this work, we introduce a noise preserving sharpening filter, referred to as NPSF, that can be used to sharpen an image while keeping the noise energy and texture in the result similar to that of the input. Furthermore, the NPSF has three user-adjustable parameters which control the sharpness and noise level in the results. We achieve this by introducing appropriately scaled noise with desirable texture to both input and ground truth images while training a DNN. We verified the performance of the NPSF for a real-world application, to sharpen CT images acquired with an extra-large (XL) focal spot and reconstructed with a high-resolution kernel. Our results demonstrate that the NPSF can sharpen images while retaining the desired noise energy and texture.

## 2. NOISE PRESERVING SHARPENING FILTER

Let  $X$  be a noise-free high-resolution image and  $Y$  be the observed blurred and noisy image. Our goal is to recover  $\tilde{X}$  from  $Y$ , where  $\tilde{X}$  is a high-resolution image which has noise energy that is similar to  $Y$  but has less blur. To do this, we train a sharpening algorithm  $f_\theta(\cdot)$  with parameters  $\theta$  by minimizing the mean squared error defined by

$$\text{MSE}_{\tilde{X}} = \mathbb{E}[||\tilde{X} - \hat{X}||^2], \quad (1)$$

where  $\hat{X}$  is given by

$$\hat{X} = f_\theta(Y). \quad (2)$$

This research is funded by GE Healthcare, Waukesha, WI, USA.

A challenge in training the proposed noise preserving sharpening filter (NPSF),  $f_\theta(\cdot)$ , is to create appropriate training pairs  $(Y_k, \tilde{X}_k)$  for  $k = 1, \dots, K$ , where  $K$  is the total number of training pairs. In the prior literature, there are two typical approaches to creating training pairs for a DNN-based sharpening algorithm.

In the *No-Noise Sharpener* approach, ground truth is taken to be a noise-free high-resolution image, and  $Y_k$  is created by blurring the ground truth image [7]. In this case, the DNN gets trained to do pure sharpening. An important disadvantage of this approach is that it does not account for the sensor noise in an observed image. Consequently, the DNN sharpener will substantially enhance the noise that is inevitably present.

In the *Denoising Sharpener* approach,  $Y_k$  is created by blurring a noise-free high-resolution ground truth image and adding noise [6]. In this case, the DNN gets trained to do both sharpening and denoising. This second approach better accounts for sensor noise in  $Y$ . However, it tends to result in deblurred images with too much noise reduction, which can result in an image,  $\hat{X}$  of (2), that lacks the texture which is highly desirable to radiologists.

Our goal is to generate training pairs,  $(Y_k, \tilde{X}_k)$ , that both account for noise in the image  $Y$  and result in an estimate  $\hat{X}$  that preserves noise energy and texture, and enhances detail. Below we describe the procedure for generating training pairs that results in the noise preserving sharpening filter.

For every  $k^{\text{th}}$  noise-free high-resolution training image  $X_k$ , we first generate the input image

$$Y_k = G(\rho) * X_k + \lambda_1 W_k, \quad (3)$$

where  $G(\rho)$  is a Gaussian filter of standard deviation  $\rho = [\rho_x, \rho_y, \rho_z]$  with  $\rho_x$ ,  $\rho_y$  and  $\rho_z$  as the standard deviation of the filter along the x, y and z direction, respectively,  $\lambda_1$  is a parameter that controls the noise energy added to the blurred image, and  $W_k$  is a noise image with desirable texture and variance  $\sigma_w^2$ .

Similarly, we generate the target image  $\tilde{X}_k$  by adding a scaled version of the **same** noise sample to  $X_k$

$$\tilde{X}_k = X_k + \lambda_2 W_k, \quad (4)$$

where  $\lambda_2$  is a parameter that determines the noise energy.

To set the values of  $\lambda_1$  and  $\lambda_2$ , we choose

$$\lambda_1 = \alpha \sqrt{\frac{\sigma_{\text{noise}}^2}{\sigma_w^2}}, \quad \lambda_2 = \beta \lambda_1, \quad (5)$$

where  $\alpha$  and  $\beta$  are user-adjustable parameters, and  $\sigma_{\text{noise}}^2$  is the noise variance of the input anticipated in the application.

Intuitively, the parameter  $\alpha$  allows one to set the standard deviation of the noise in the training input, and  $\beta$  allows one to control the standard deviation of the noise in the ground truth. Typically,  $\alpha = 1.0$ ; so the noise variance in the training input

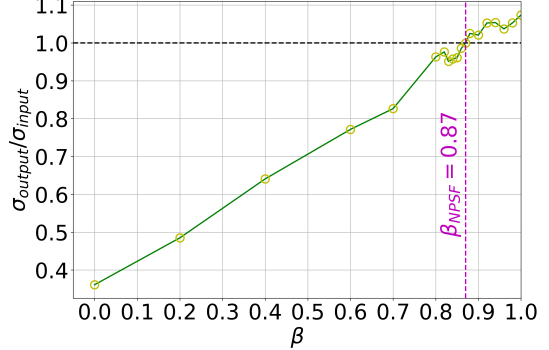


**Fig. 1:** Effect of  $\beta$  on noise in the sharpened image.

matches the noise variance anticipated in the application. The value of  $\beta$  is then adjusted to meet the noise preserving condition, i.e., that the noise variance of the DNN output matches to the noise variance of the input. This is done experimentally with the data that is typical for the application.

Fig. 1 plots the ratio of the output to input noise standard deviation measured experimentally as a function of increasing  $\beta$ . Notice that larger values of  $\beta$  result in noisier sharpened images. In particular,  $\beta_{\text{NPSF}}$  corresponds to the parameter value so that  $\sigma_{\text{output}}^2 = \sigma_{\text{input}}^2$ , i.e., where the output noise variance is matched to the input noise variance. For this example,  $\beta_{\text{NPSF}} = 0.87$  for the setting in Fig. 1 ( $\rho = [0.34, 0.34, 0.22]$  mm,  $\alpha = 1$ ).

The parameter  $\alpha$  determines the amount of noise added to the training pairs and consequently, can be used to control the suppression of other artifacts such as aliasing in the results. Larger values of  $\alpha$  result in fewer artifacts, but with the trade-off of somewhat less detail. Finally, the parameter  $\rho$  controls the level of sharpening. A larger value of  $\rho$  simulates higher blur while training and thus producing sharper results.

### 3. EXPERIMENTAL RESULTS

We evaluate the NPSF for the task of sharpening CT images that have been captured using an extra-large (XL) focal spot size and reconstructed with a high-resolution kernel. We compare to results obtained with the No-Noise Sharpener and the Denoising Sharpener of Section 2, and all three networks use the CNN architecture of [14].

#### 3.1. Methods

For training, high-resolution images are acquired with a small focal spot. Then noise-free high-resolution realizations,  $X_k$ , are obtained by averaging multiple scans of the same phantom. We used 2 phantoms to get 4 training images. To obtain the noise realizations,  $W_k$ , 3 water phantoms are scanned.

The training and testing data was collected on a GE Revolution CT scanner (GE Healthcare, WI, USA). The acquisition and reconstruction settings used are listed in Table (1).

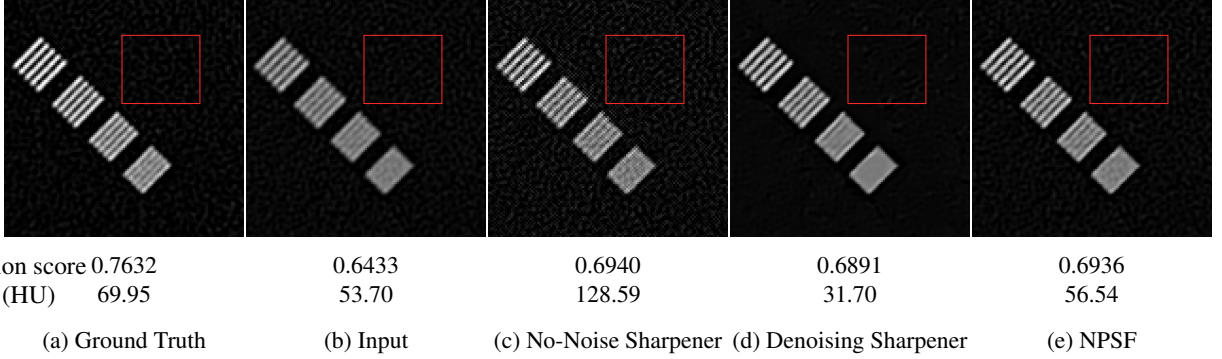


**Fig. 2:** Results for Catphan. NPSF with  $\rho = [0.34, 0.34, 0.22]$  mm,  $\beta_{NPSF} = 0.87$ ,  $\alpha = 1$ . Display window [0, 2000] HU.

All exams except water phantoms are reconstructed with the Bone+ kernel, a high-resolution reconstruction kernel option available on the GE scanner designed to preserve more edge detail. The exams are reconstructed to a slice thickness of 0.625 mm and interval 0.3125 mm. Water phantoms are reconstructed with filtered backprojection (FBP) to a slice thickness of 0.625mm. The reconstructed training volumes were broken into  $128 \times 128 \times 7$  patches, with the patches randomly partitioned as 97% for training and 3% for validation.

**Table 1:** Training and test exams

	Exams	Focal spot	Dosage (kVp/mA)	DFOV (cm)
Train	High resolution	small	120/320	25
	Water phantom	small	120/350	40
Test	Catphan (phantom)	XL	100/880	15
	Catphan ground truth	small	100/245	15
	Exam 1 (clinical)	XL	120/530	15

To train the network, we used the Adam optimizer [15] with an initial learning rate of 0.001 and a mini-batch size of 32. The learning rate was reduced by a factor of 4 if no improvement in validation loss occurred for 5 epochs, and the training was stopped if the validation loss was not improved for 16 consecutive epochs. The network was implemented in Keras [16] and trained with an NVIDIA Tesla V100 GPU.

### 3.2. Results & Discussion

Fig. 2 compares results for the Catphan exam acquired using the Catphan 700 phantom [17]. The figure shows the ground truth and input, along with results for the conventional and NPSF methods. The resolution section of the phantom consists of line pairs arranged at various spatial frequencies, and the background region can be used to assess the noise amplitude and texture. Under each image there is a measure of resolution and noise. The resolution score measures the variation of the line-pairs to the known variation of the phantom;

so an ideal resolution score should be 1.0, with lower values indicating reduced resolution. For noise, the standard deviation (std) in HU units for the ROI marked has been reported.

As seen in Fig. 2 (c), the No-Noise Sharpener produces blocky artifacts on line pairs and areas around them. Furthermore, the noise has increased by a factor of 2.4 as compared to the input image. Also notice, that the Denoising Sharpener removes too much noise, resulting in a loss of texture in regions such as the finest line pairs.

Alternatively, the proposed NPSF result of Fig. 2(e) matches the input noise level while increasing the resolution. This retains appropriate texture and detail while sharpening.

Fig. 3 shows the results for the Exam 1. As this is a clinical exam, its ground truth is not available. The  $\beta$  parameter is tuned for the noise preserving case. As seen in the second and third columns, the No-Noise Sharpener drastically increases noise and artifacts while the Denoising Sharpener loses texture. Alternatively, the NPSF (with  $\alpha = 1.0$  or  $\alpha = 1.6$ ) sharpens the input image while keeping the noise level and texture similar to that of the input. This is further evident from the second row which shows a zoomed inner ear portion.

The fifth column of Fig. 3 shows the effectiveness of  $\alpha$  in controlling aliasing artifacts in the sharpened images. Magenta arrows Fig. 3 (f) and (k) point to areas in the input which are heavily affected by such artifacts. The No-Noise Sharpener, Denoising Sharpener and NPSF with  $\alpha$  as 1 have sharpened these artifacts too, making them worse. However, in contrast to conventional methods, increasing  $\alpha$  to 1.6 in NPSF reduces the aliasing artifacts in the results to a great extent while having only a small effect on the sharpness.

Fig. 4 shows NPSF ( $\alpha = 1$ ) results for an input with noise std of 74.63 HU. The number below each image in the first row is the noise std for the respective result. The noise std is computed using multiple uniform regions in the volume. Residual images in the second row show that higher  $\rho$  achieves more sharpening. Most importantly, the noise measurements show that if  $\beta$  is set appropriately then the NPSF can keep the noise energy in the result similar to that of the input. In addition to the noise preserving case, Fig. 1 showed

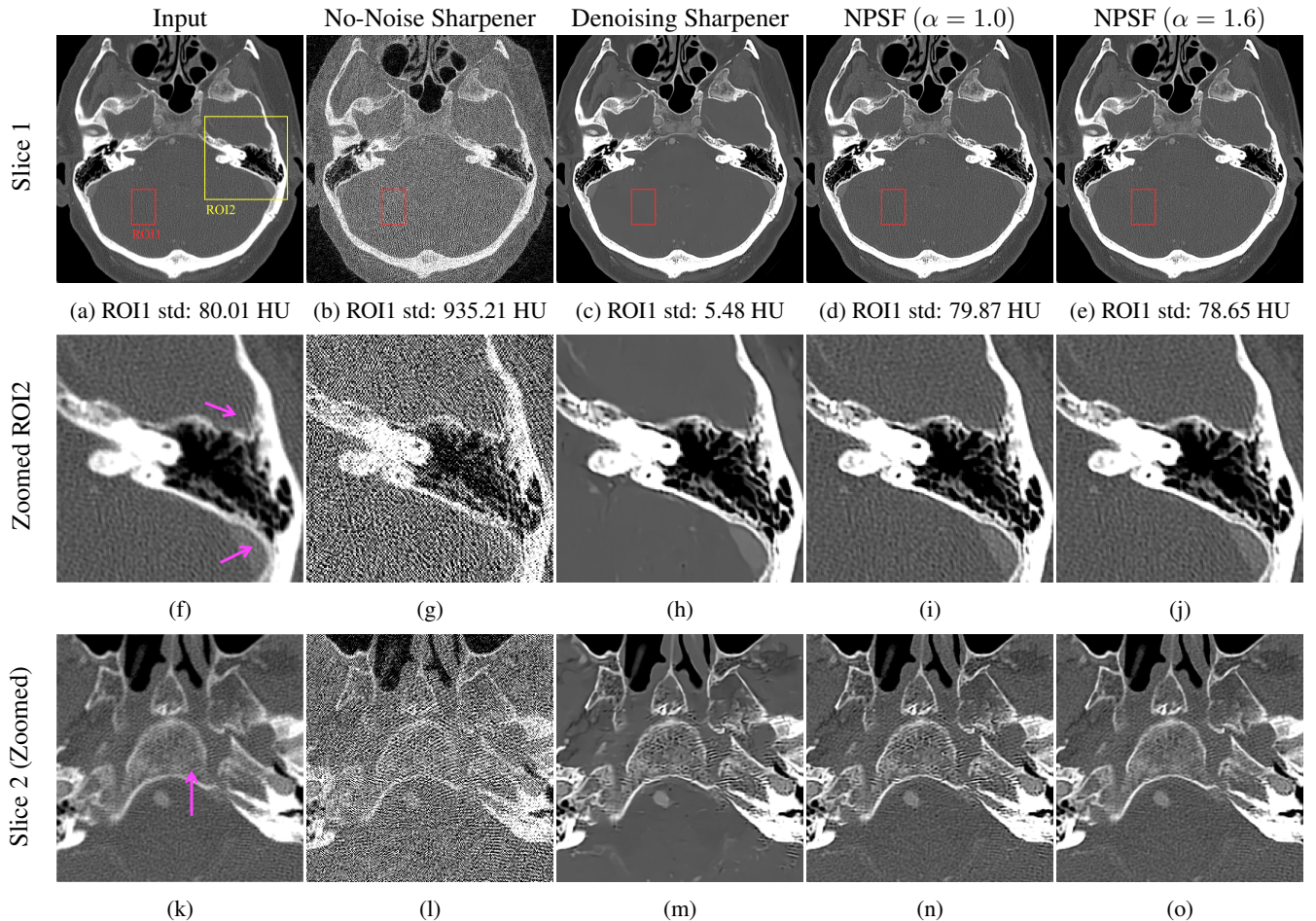


**Fig. 3:** Results for Exam 1. NPSF with  $\rho = [0.54, 0.54, 0.34]$  mm,  $\beta_{NPSF} = 0.98$ . Display window = [-650, 1350] HU.

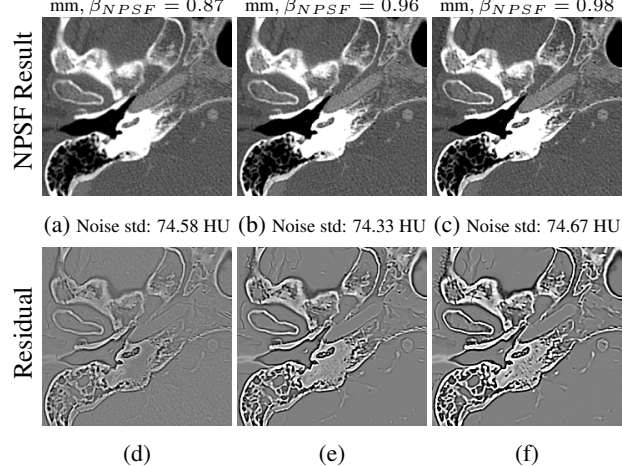


**Fig. 4:** NPSF noise preserving case for different  $\rho$ . Display window: Results [-650, 1350] HU, Residuals [-200, 200] HU.

that  $\beta$  can be set to get the desired noise level in the result.

#### 4. CONCLUSION

We propose a noise preserving sharpening filter (NPSF) which sharpens CT images while retaining desirable noise level and texture. To achieve this, the NPSF is trained with image pairs that contain appropriately scaled noise in both the blurred input and the high-resolution ground truth. Thereby NPSF can control the level of sharpness and noise in the results with three user-adjustable parameters. The performance of NPSF has been verified for a clinical application of resolution improvement of scans acquired with an XL focal spot and reconstructed with a high-resolution kernel. Quantitative and qualitative evaluations show that NPSF outperforms the conventional approaches.

#### 5. ACKNOWLEDGMENT

We thank Karen Procknow for her valuable clinical feedback.

## 6. REFERENCES

- [1] B. Li, G. B Avinash, and J. Hsieh, “Resolution and noise trade-off analysis for volumetric CT,” *Medical physics*, vol. 34, no. 10, pp. 3732–3738, 2007.
- [2] M. Jiang, G. Wang, M.W. Skinner, J.T. Rubinstein, and M.W. Vannier, “Blind deblurring of spiral CT images,” *IEEE Transactions on Medical Imaging*, vol. 22, no. 7, pp. 837–845, 2003.
- [3] J.-B. Thibault, K. D. Sauer, C. A. Bouman, and J. Hsieh, “A three-dimensional statistical approach to improved image quality for multislice helical CT,” *Medical Physics*, vol. 34, no. 11, pp. 4526–4544, 2007.
- [4] R. Zhang, J.-B. Thibault, C. A. Bouman, K. D. Sauer, and J. Hsieh, “Model-based iterative reconstruction for dual-energy X-Ray CT using a joint quadratic likelihood model,” *IEEE Transactions on Medical Imaging*, vol. 33, no. 1, pp. 117–134, 2014.
- [5] J. Kuntz, J. Maier, M. Kachelrieß, and S. Sawall, “Focal spot deconvolution using convolutional neural networks,” in *Medical Imaging 2019: Physics of Medical Imaging*. International Society for Optics and Photonics, 2019, vol. 10948, p. 109480Q.
- [6] D. Yim, B. Kim, and S. Lee, “A deep convolutional neural network for simultaneous denoising and deblurring in computed tomography,” *Journal of Instrumentation*, vol. 15, no. 12, pp. P12001, 2020.
- [7] C. Dong, C. C. Loy, K. He, and X. Tang, “Image super-resolution using deep convolutional networks,” *IEEE Transactions on Pattern Analysis and Machine Intelligence*, vol. 38, no. 2, pp. 295–307, 2016.
- [8] M. Chen, Y. Chang, S. Cao, and L. Yan, “Learning blind denoising network for noisy image deblurring,” in *ICASSP 2020 - 2020 IEEE International Conference on Acoustics, Speech and Signal Processing (ICASSP)*, 2020, pp. 2533–2537.
- [9] K. Zhang, W. Zuo, and L. Zhang, “Learning a single convolutional super-resolution network for multiple degradations,” in *Proceedings of the IEEE Conference on Computer Vision and Pattern Recognition*, 2018, pp. 3262–3271.
- [10] J. Chi, Y. Zhang, X. Yu, Y. Wang, and C. Wu, “Computed tomography (CT) image quality enhancement via a uniform framework integrating noise estimation and super-resolution networks,” *Sensors*, vol. 19, no. 15, pp. 3348, 2019.
- [11] J. M. Wolterink, T. Leiner, M. A. Viergever, and I. Išgum, “Generative adversarial networks for noise reduction in low-dose CT,” *IEEE Transactions on Medical Imaging*, vol. 36, no. 12, pp. 2536–2545, 2017.
- [12] W. Dong, L. Zhang, G. Shi, and X. Wu, “Image deblurring and super-resolution by adaptive sparse domain selection and adaptive regularization,” *IEEE Transactions on Image Processing*, vol. 20, no. 7, pp. 1838–1857, 2011.
- [13] C. You, G. Li, Y. Zhang, X. Zhang, H. Shan, M. Li, S. Ju, Z. Zhao, Z. Zhang, W. Cong, M. W. Vannier, P. K. Saha, E. A. Hoffman, and G. Wang, “CT super-resolution GAN constrained by the identical, residual, and cycle learning ensemble (GAN-CIRCLE),” *IEEE Transactions on Medical Imaging*, vol. 39, no. 1, pp. 188–203, 2020.
- [14] K. Zhang, W. Zuo, Y. Chen, D. Meng, and L. Zhang, “Beyond a gaussian denoiser: Residual learning of deep cnn for image denoising,” *IEEE Transactions on Image Processing*, vol. 26, no. 7, pp. 3142–3155, 2017.
- [15] D. P. Kingma and J. Ba, “Adam: A method for stochastic optimization,” in *3rd International Conference on Learning Representations, ICLR 2015*, 2015.
- [16] F. Chollet et al., “Keras,” <https://keras.io>, 2015.
- [17] “Catphan 700 manual,” Product guide, The Phantom Laboratory, 2016.